

MicroRNA-101 Regulates Multiple Developmental Programs to Constrain Excitation in Adult Neural Networks

Highlights

- MiR-101 orchestrates early network development to limit excitation in the adult
- Transient miR-101 blockade leads to hyper-excitability and memory deficits
- MiR-101 targets NKCC1 to facilitate the GABA switch and constrains dendrites
- Ank2 and Kif1a are targeted by miR-101 to limit formation of excitatory synapses

Authors

Giordano Lippi, Catarina C. Fernandes,
Laura A. Ewell, ..., Giuseppe Biagini,
Gene W. Yeo, Darwin K. Berg

Correspondence

gliippi@ucsd.edu (G.L.),
dberg@ucsd.edu (D.K.B.)

In Brief

Lippi et al. discovered that microRNA-101 regulates multiple genetic programs in parallel to orchestrate a major transition in early development, ensuring that adult neural circuits display appropriate excitability. MicroRNA-101 blockade induces hyper-excitability and memory deficits characteristic of numerous neurodevelopmental disorders.

MicroRNA-101 Regulates Multiple Developmental Programs to Constrain Excitation in Adult Neural Networks

Giordano Lippi,^{1,5,*} Catarina C. Fernandes,¹ Laura A. Ewell,¹ Danielle John,¹ Benedetto Romoli,² Giulia Curia,² Seth R. Taylor,¹ E. Paxon Frady,¹ Anne B. Jensen,¹ Jerry C. Liu,¹ Melanie M. Chaabane,¹ Cherine Belal,¹ Jason L. Nathanson,³ Michele Zoli,² Jill K. Leutgeb,^{1,4} Giuseppe Biagini,² Gene W. Yeo,³ and Darwin K. Berg^{1,*}

¹Division of Biological Sciences, University of California, San Diego, La Jolla, CA 92093, USA

²Department of Biomedical, Metabolic, and Neural Sciences, Center for Neuroscience and Neurotechnology, University of Modena and Reggio Emilia, Modena 41125, Italy

³Institute for Genomic Medicine

⁴Center for Neural Circuits and Behavior

University of California, San Diego, La Jolla, CA 92093, USA

⁵Lead Contact

*Correspondence: glli@ucsd.edu (G.L.), dberg@ucsd.edu (D.K.B.)

<http://dx.doi.org/10.1016/j.neuron.2016.11.017>

SUMMARY

A critical feature of neural networks is that they balance excitation and inhibition to prevent pathological dysfunction. How this is achieved is largely unknown, although deficits in the balance contribute to many neurological disorders. We show here that a microRNA (miR-101) is a key orchestrator of this essential feature, shaping the developing network to constrain excitation in the adult. Transient early blockade of miR-101 induces long-lasting hyperexcitability and persistent memory deficits. Using target site blockers *in vivo*, we identify multiple developmental programs regulated in parallel by miR-101 to achieve balanced networks. Repression of one target, NKCC1, initiates the switch in γ -aminobutyric acid (GABA) signaling, limits early spontaneous activity, and constrains dendritic growth. Kif1a and Ank2 are targeted to prevent excessive synapse formation. Simultaneous de-repression of these three targets completely phenocopies major dysfunctions produced by miR-101 blockade. Our results provide new mechanistic insight into brain development and suggest novel candidates for therapeutic intervention.

INTRODUCTION

Balanced excitation is a critical feature of properly functioning neural circuits. Aberrant activity is characteristic of numerous neurological disorders, including autism spectrum disorder (ASD), Rett syndrome, schizophrenia, and epilepsy (Belforte et al., 2010; Chao et al., 2010; Dzhala et al., 2005; Rubenstein and Merzenich, 2003; Yizhar et al., 2011; Zoghbi and Bear,

2012). In rodents, formative events in the first few weeks of post-natal life specify the ratio of excitatory and inhibitory input (E/I) and determine the excitability of neural circuits for the adult (Ben-Ari, 2002; Blankenship and Feller, 2010). During this time, the developing nervous system transitions from an initial period of rapid growth and exuberant synapse formation to a period during which circuits undergo refinement and consolidation (Blankenship and Feller, 2010; Kirkby et al., 2013). Disruptions in the timing or sequence of events comprising the growth phase and transition to consolidation can produce aberrant levels of excitation in the adult. How this complex process of network construction is guided to ensure proper excitation is largely unknown.

MicroRNAs (miRNAs) are strong candidates for coordinating complex developmental processes (Bian and Sun, 2011; Yoo et al., 2009). They are short non-coding RNAs that act as post-transcriptional regulators of gene expression (Bartel, 2004; Guo et al., 2010) by binding mRNAs containing a miRNA recognition element (MRE). A single miRNA can target hundreds of different mRNAs, orchestrating epigenetic regulation of large combinations of gene products and facilitating developmental switches (Makeyev et al., 2007; McNeill and Van Vactor, 2012). Little is known, however, about possible miRNA involvement in post-natal brain development and long-term effects.

Here we show that miR-101 regulates multiple post-natal developmental programs in parallel to constrain excitatory activity in the adult. Using target site blockers *in vivo*, we identify the molecular mechanisms used by miR-101 to produce balanced networks. It represses NKCC1 to initiate maturation of GABAergic signaling, to limit spontaneous synchronized activity, and to prevent excessive dendritic growth. A second developmental program involves repression of Kif1a and Ank2 to constrain excessive assembly of pre-synaptic components and reduce the density of glutamatergic synapses. Remarkably, simultaneous protection of all three targets recapitulates the core of the phenotype induced by miR-101 blockade.

RESULTS

MiR-101 Is a Potential Master Regulator of Network Formation

To identify miRNAs orchestrating the complex series of events occurring during network formation, we performed small RNA sequencing of the mouse hippocampus on post-natal day 12 (P12). The hippocampus was chosen because of its known function and well defined circuitry; P12 was chosen because it is within a critical developmental window (Liu et al., 2006). The miRNAs obtained were then ranked according to the following criteria. First, abundance, expressed as percentage of total counts. Highly abundant miRNAs are more likely to have prominent roles. Second, upregulation during post-natal development. miRNA levels rise when their function becomes necessary. Accordingly, we used qPCR to quantify the levels of top miRNA candidates in the hippocampus from embryonic day 16 (E16) to adult. Third, enrichment of miRNAs and mRNAs in Argonaute (Ago) complexes (the effector of miRNA function). We explored existing databases of Ago-miRNA-mRNA interactions that list the abundance of miRNAs and their predicted mRNA targets (Boudreau et al., 2014; Chi et al., 2009). miRNAs were prioritized when they were enriched in Ago complexes and had predicted target transcripts (based on MRE) with known roles in neuronal development, and those targets were also abundant in the complexes. Of those, miR-101a and b stood out as the most promising. MiR-101a and b are highly expressed on P12 (Figure S1A, available online), increase 2- and 3-fold, respectively, during the relevant developmental window of E16–P12 (Figures S1B and S1C), represent some of the most abundant miRNAs in Ago-miRNA-mRNA complexes in the cortex on P13, and have validated targets that are crucial for neuronal differentiation (Figure S1D). Notably, miR-101 is expressed not only in pyramidal neurons but also in interneurons (Figure S2A) and in non-neuronal cell types (Figures S2B and S2C).

To assess the role of miR-101a and b in mediating early events in brain development, we performed a localized transient inhibition by injecting a fluorescein-tagged locked nucleic acid (LNA) antagonist for miR-101b (a-101.F) bilaterally into the dorsal hippocampus of P2 pups (Figure 1A). Sensor assays and qPCR experiments showed that the antagonist efficiently and selectively inhibited both miR-101a and b for up to 9 days compared with a control LNA (a-Ctrl) and subsequently subsided (Figures S2D–S2F and S3). Additional controls were performed to validate the antagonist and exclude that base composition or LNA length were responsible for the phenotype observed (Figures S2G–S2I). The timing and transience of the inhibition were significant. It meant that any network defects persisting into adulthood must result from having interrupted early actions of miR-101 that normally have long-lasting effects. Although miR-101 is also highly expressed in the adult (Figures S1B and S1C), acute actions during adulthood would not have been compromised by application of a-101.F on P2. Similarly, injection on P2 would not perturb miR-101 actions during embryogenesis, e.g., effects on early cell proliferation and migration.

Transient MiR-101 Inhibition in Early Life Produces Hyper-excitatory Networks in the Adult

To determine whether transitory inhibition of miR-101 during post-natal development creates long-lasting changes in circuit function, we tested the levels of excitability in multiple areas of the hippocampus with an array of techniques. First, we measured hippocampal single unit activity in freely behaving adult mice in an intact network long after miR-101 inhibition ended. During periods when animals were resting, pyramidal neurons had significantly elevated firing rates in a-101.F-treated animals compared with a-Ctrl-treated controls (Figures 1B–1D and S4A–S4C). This increase in baseline activity is consistent with hyper-excitatory networks.

Further evidence for increased excitation came from recordings of spontaneous excitatory postsynaptic currents (sEPSCs) in CA3 pyramidal neurons in acute hippocampal slices from young adults (P40). Both the frequency and amplitude of excitatory events were significantly increased by a-101.F compared with a-Ctrl (Figures 1E–1G). Even more striking was the appearance of spontaneous high-frequency burst discharges that resembled spontaneous seizure-like events (SLEs) seen in half of the slices from a-101.F-treated animals (Figure 1E, bottom).

To measure activity more broadly, we injected P2 pups with an adeno-associated virus encoding the calcium indicator GCaMP6f along with a-101.F and examined the dentate gyrus (DG), which is the main source of excitatory fibers to CA3 pyramidal neurons. Spontaneous calcium transients in acute P37–P40 slices were imaged using confocal microscopy (Figures 1H, 1I, S4D, and S4E). DG neurons from a-101.F-treated animals exhibited increased activity compared with a-Ctrl (Figure 1J). Both the percentage of spontaneously active DG neurons and the frequency of calcium transients per active cell were increased (Figures 1K and 1L, bars labeled P2). In addition, neurons from a-101.F-treated animals occasionally showed prolonged bursts of excitatory activity (Figure 1J, bottom). Importantly, acute injections of a-101.F on P30, 8–10 days before calcium imaging, did not alter DG activity (Figures 1K and 1L, bars labeled P30). This is consistent with the earlier demonstration that P2 injection of a-101.F achieves only a transient blockade. Accordingly, miR-101 must act during post-natal development to subsequently determine excitability in the adult. Acute actions of miR-101 in the adult have other consequences (Lee et al., 2008; Vilardo et al., 2010).

Because anomalous bursts of excitatory activity were detected in a-101.F-treated animals (Figures 1E and 1J), we asked whether the network presented major pathological features. Both the pentylenetetrazole (PTZ) infusion test and Timm staining in the DG showed no difference between a-101.F-treated animals and littermate controls (Figures S4F–S4H). Local field potential (LFP) video monitoring revealed that one a-101.F-treated animal of seven showed inter-ictal spikes and stage III seizures (data not shown) whereas all other animals did not. The maximal electroshock seizure (MES) test suggested that evoked seizures, although of similar severity, lasted significantly longer in a-101.F-treated animals than in a-Ctrl controls (Figures S4I–S4K). Together, the data indicate that, in a-101.F animals, the network is clearly prone to hyper-excitability but does not exhibit a full epileptic phenotype.

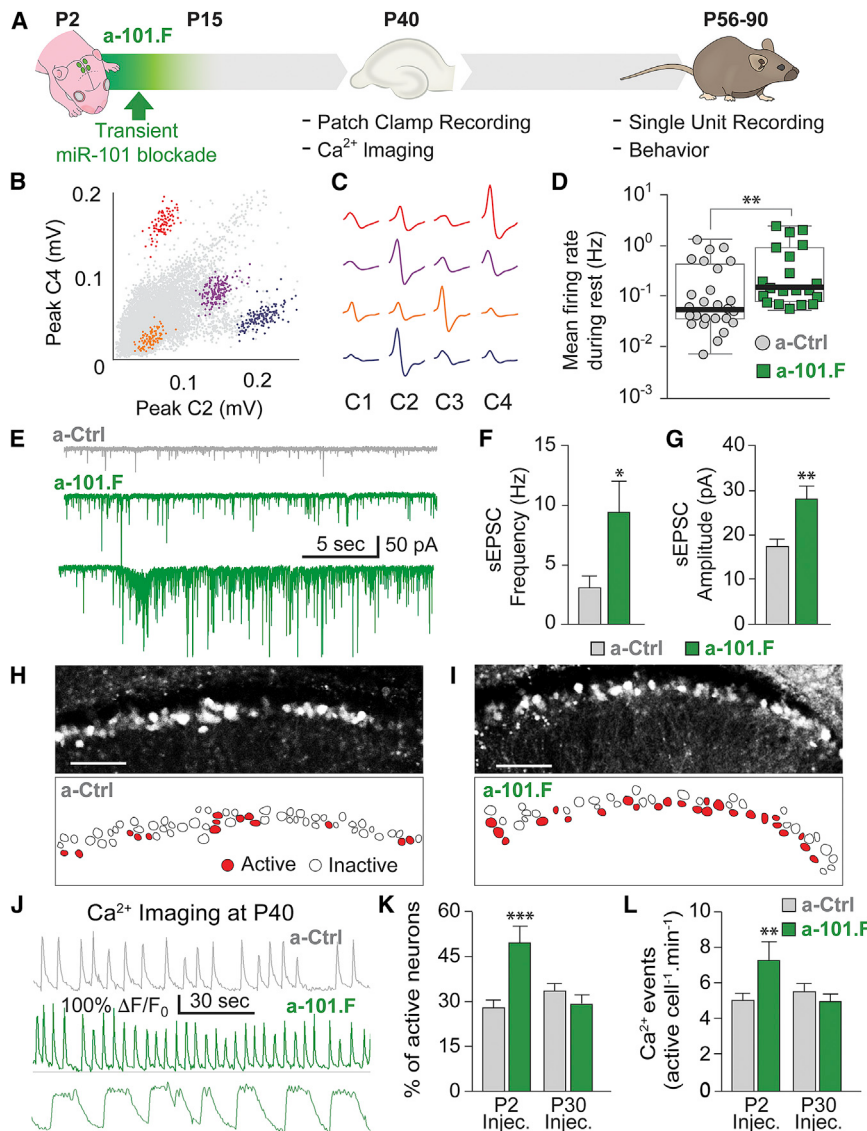


Figure 1. Transitory MiR-101 Inhibition Early in Development Induces Hyper-excitable Networks in the Young Adult

(A) Schematic of the time course for miR-101 inhibition *in vivo* (green) and follow-up tests to assess consequences.

(B and C) Single-unit recordings from the hippocampus in freely behaving mice (channels C1–C4) and scatterplots of relative waveform peak amplitudes (B) with mean waveforms plotted (C).

(D) Mean spike rates for single units in a-101.F-versus a-Ctrl-treated mice. Median values, bold black line; inter-quartile range, box edges.

(E) sEPSC recordings in acute slices showing increased spontaneous excitatory activity in a-101.F-treated neurons (versus a-Ctrl controls) on P40 (top two traces). Spontaneous high-frequency burst discharges were seen in half of the slices from a-101.F-treated animals (bottom trace).

(F and G) Quantification of sEPSCs in CA3 reveals an increase in frequency (F) and amplitude (G) in a-101.F-treated neurons.

(H–L) Confocal imaging of spontaneous calcium transients on P40.

(H and I) Images of DG granule cells virally expressing GCaMP6f (top) and a scheme of the cells in the same field of view (bottom) color-coded for active (red) and inactive (white) cells for a-Ctrl (H) and a-101.F-treated animals (I) after injection on P2. Scale bars, 100 μ m.

(J) Representative calcium traces showing increases in event frequency (center) and prolonged transients (bottom) in a-101.F-treated animals compared with controls (top). ΔF , variation in fluorescence; F_0 , baseline fluorescence.

(K and L) Quantification of calcium activity showed an increase in the number of active cells (K) and in the frequency of events (L) in slices from P40 animals injected on P2 (P2 Injec.) but not when injected on P30 (P30 Injec.).

Bar graphs (except D): mean \pm SEM; Student's t test; Mann-Whitney U test (D). * p < 0.05, ** p < 0.01, *** p < 0.001.

Transient Blockade of MiR-101 Early in Development Causes Memory Deficits in the Adult

In many neurodevelopmental disorders, hyper-excitability is often accompanied by cognitive impairment. To determine whether the dysfunctions imposed by transitory miR-101 blockade correlate with long-lasting behavioral change, we tested young adult mice in a battery of tasks that probe hippocampal function. In the fear conditioning test, young adult mice that received a-101.F on P2 froze less in the context in which they received a foot shock (Figures 2A and 2B). This is consistent with the classical notion that formation of contextual memories is hippocampus-dependent (Curzon et al., 2009). Importantly, memory of the cue tone, which is, instead, amygdala-dependent, was not altered by miR-101 blockade. The spontaneous alternation assay requires a functionally intact dorsal hippocampus and is used to test spatial working memory in young rodents. Compared with controls, animals that received a-101.F completed fewer correct alternations, suggesting that they

were less likely to remember the arm of the symmetrical Y maze that was last visited (Figures 2C–2E). Animals that received a-101.F also showed impairments in the object/place test, which measures the ability of the animals to remember the location of one of two identical objects (Figures 2F–2I). These data suggest that hippocampus-dependent contextual, working, and spatial memory were impaired in a-101.F-treated mice compared with controls. No significant differences were observed in the open field and the elevated plus maze tests, confirming that the observed memory effects were not a result of changes in anxiety levels or in general exploratory behavior (Figures 2J and 2K).

Taken together, the results show that miR-101 function in the first 2 weeks of post-natal development is critical for subsequent neural circuit function. Transient loss of miR-101 regulation in the dorsal hippocampus has long-lasting consequences, leading to a hyper-excitable network and cognitive deficits. The profound effects of miR-101 blockade on network excitability in the adult emerge from disinhibiting mRNA targets during early post-natal

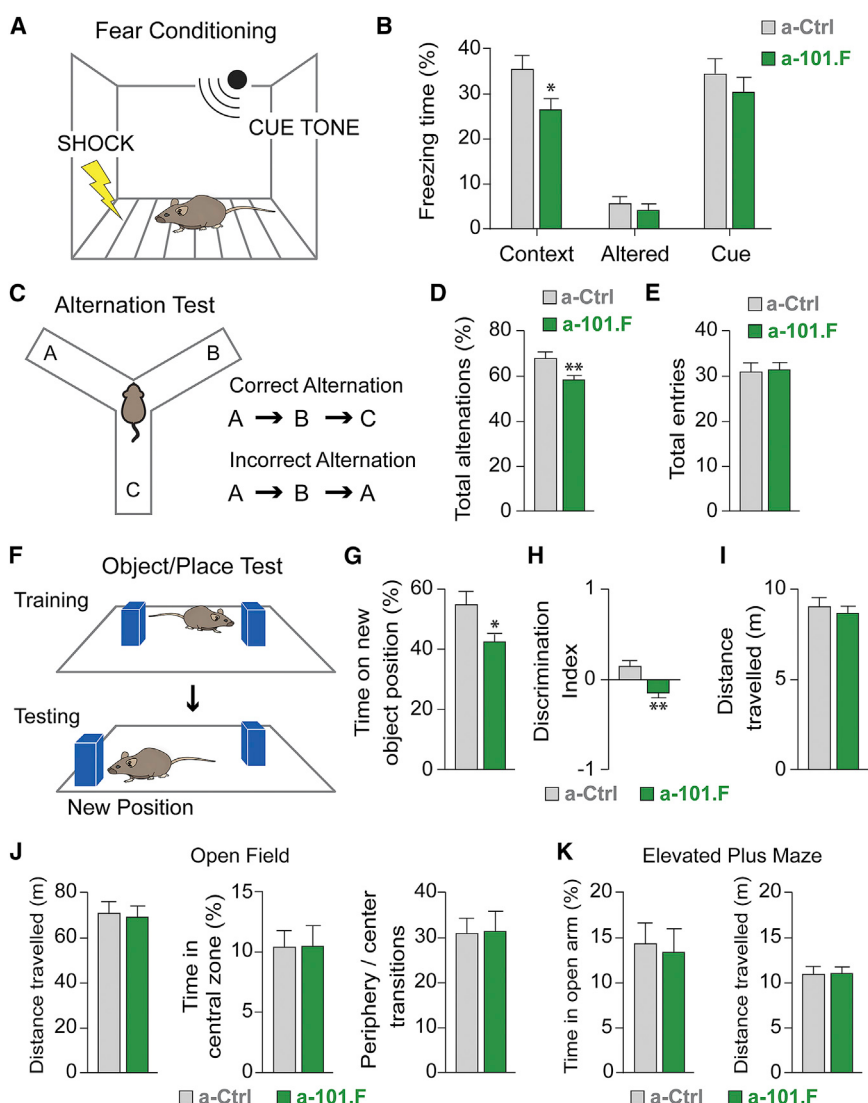


Figure 2. Transient MiR-101 Blockade Early in Development Produces Memory Impairment in the Adult

(A) Fear conditioning test pairing shock with context and tone cue.

(B) Animals receiving a-101.F spend less time freezing when re-exposed to the context where they received the shock, indicating impaired association between context and shock. Exposure to a different cage (Altered) induced little freezing in either group.

(C) Alteration test involving a symmetrical Y maze with examples of correct and incorrect alternations.

(D and E) Animals treated with a-101.F performed fewer correct alternations than controls while traveling the same distance (E), suggesting impaired spatial working memory.

(F) Object/place test comparing time spent at the new versus old object position.

(G–I) Animals with a-101.F spent less time at the new object position (G and H) while traveling the same distance (I), suggesting impaired spatial memory. The discrimination index (H) suggests that the animals have a modest bias toward the location of the object that was not moved.

(J) Open field tests showed that a-101.F treatment does not alter the distance traveled by the mice (left), time spent in the central zone of the arena (center), or number of transitions from the periphery to the center of the arena (right). The miR-101 antagonist does not, therefore, alter exploratory behavior or novelty-induced anxiety levels.

(K) Elevated plus maze test. No significant difference was detected between the groups in time spent in the open arms (left, index of anxiety) or total distance traveled (right).

Mean \pm SEM, Student's t test, Welch's test (H); * $p < 0.05$, ** $p < 0.01$.

life. Identifying such targets will help to understand the developmental programs that converge to establish a balanced network.

MiR-101 Targets NKCC1 to Facilitate the GABA Switch, a Critical Event in Development

To identify the mechanisms by which miR-101 affects the assembly of balanced circuits, we tested individual candidate mRNA targets. We compiled a list of potential miR-101 targets, combining TARGETSCAN predicted interactions with existing high-throughput sequencing of RNA isolated by cross-linking immunoprecipitation (HITS-CLIP) databases from both the mouse cortex on P13 (Chi et al., 2009) and the human cortex (Boudreau et al., 2014). We selected 17 putative miR-101 targets most frequently associated in vivo with the Ago-miRNA-mRNA complexes. We then used qPCR to determine which candidates decreased in the hippocampus between P7 and P11 (low P11-to-P7 ratio), as expected in response to the miR-101 increase, and, conversely, which increased in response to miR-101 blockade by a-101.F, as expected for a de-repressed target.

A final selection criterion was based on the encoded protein being relevant for neural development. Seven top candidate mRNAs emerged (Table S1).

Most promising was the chloride importer NKCC1 because it declines during the second week of post-natal life in rodents and, along with an increase in the chloride exporter KCC2, is responsible for maturation of GABAergic signaling, rendering it inhibitory (Ben-Ari, 2002; Blankenship and Feller, 2010; Rivera et al., 1999). Disruption of the GABA switch during development has profound consequences for network excitability and E/I (Cancedda et al., 2007; Chen and Kriegstein, 2015; Deidda et al., 2015; Dzhala et al., 2005; He et al., 2014; Liu et al., 2006). What causes NKCC1 to decline, however, has long been the focus of investigation but remains unknown. Because the NKCC1 mRNA contains a predicted miR-101 MRE, we tested the hypothesis that miR-101 drives maturation of GABAergic signaling by repressing NKCC1 and that disrupting the timing of the GABA switch causes the hyper-excitability observed in a-101.F-treated animals.

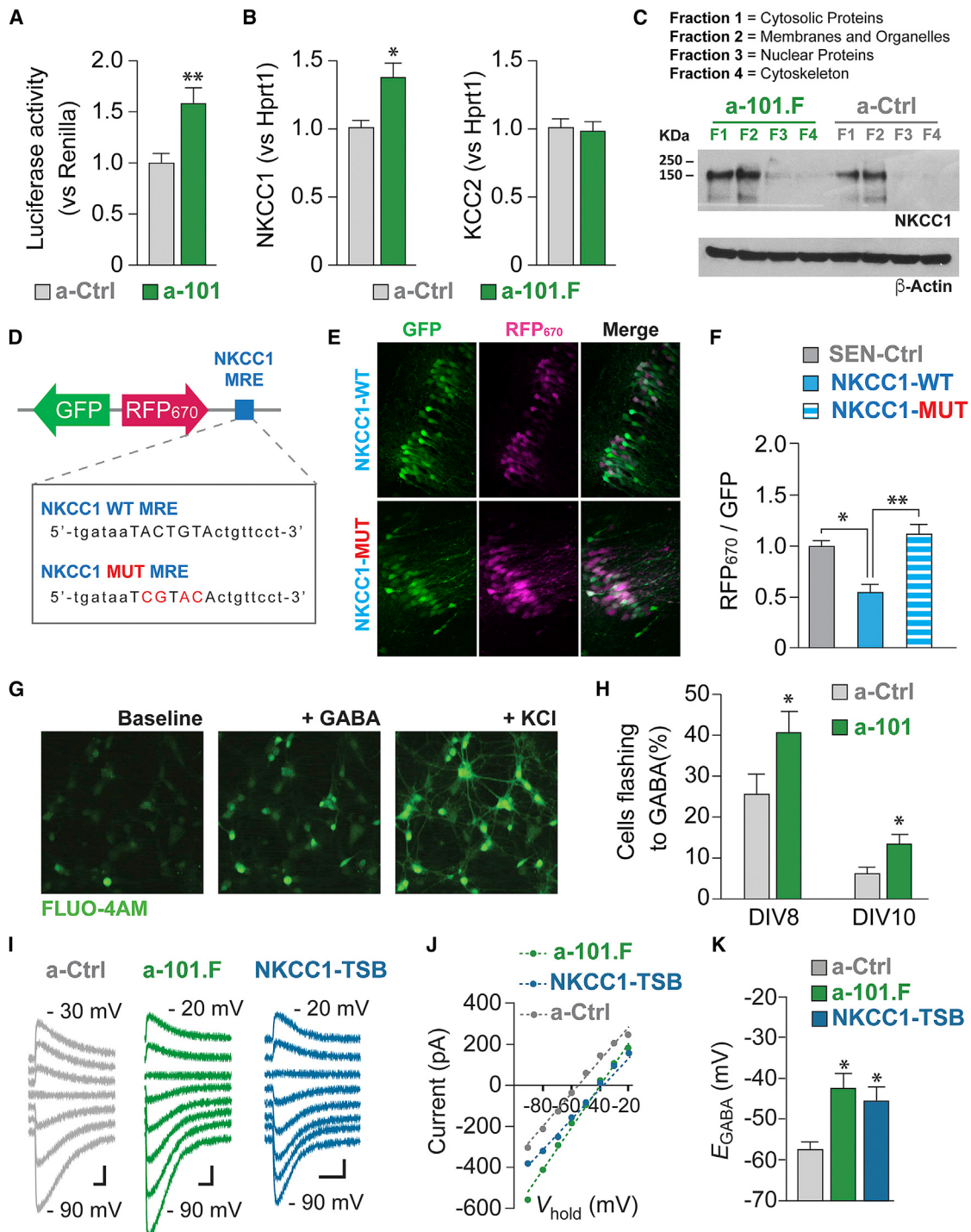


Figure 3. MiR-101 Shapes Network Development in Part by Targeting NKCC1

(A) HEK cells expressing a luciferase construct encoding the 3' UTR of NKCC1 showed increased luciferase activity (normalized for *Renilla* activity) when co-transfected with an a-101 construct.

(B) Injection of a-101.F on P2 increased NKCC1 mRNA levels in vivo (left, normalized for *Hprt1*) but did not change KCC2 levels (right), as quantified by qPCR on P8.

(C) Western blot analysis confirmed increased NKCC1 levels both in cytosolic protein and membrane/organelle fractions from P8 acute hippocampal slices of animals treated with a-101.F on P2 (four to five slices from the dorsal hippocampus from 12–14 animals). Quantification of band intensity on western blots

(legend continued on next page)

To determine whether miR-101 is critical for the decline in NKCC1 during development, we first employed cell culture. Cells expressing a luciferase construct containing the NKCC1 3' UTR showed increased luciferase activity when treated with a-101 (a-101.F without a fluorescent tag) compared with a-Ctrl-treated cells (Figure 3A). Further, a-101.F increased both NKCC1 messenger and protein levels *in vivo*, indicating that endogenous miR-101 directly targets the NKCC1 3' UTR to degrade the mRNA (Figures 3B and 3C). In contrast, KCC2 levels were not changed by miR-101 blockade (Figure 3B). Sensor assays using wild-type and mutated sequences helped confirm the MRE in the NKCC1 3' UTR that miR-101 binds to repress its translation (Figures 3D–3F). Experiments in cell culture confirmed the effect of preventing miR-101 regulation of NKCC1. Patch-clamp recording from primary neuron cultures transfected with a-101 indicated that many more neurons displayed a depolarized reversal potential for GABA (E_{GABA}), as seen in responses to pico-spritzed application of GABA, at a time when the gradient should have matured to make GABA inhibitory (Figure S5A). Consistent with this, neurons transfected with a-101 showed a much greater likelihood of displaying a depolarizing response to GABA, as monitored with a calcium-dependent fluor, than those receiving a-Ctrl (Figures 3G, 3H, and S5B).

To assess the effects of miR-101 on E_{GABA} under conditions where the neuronal connections were more similar to those *in vivo*, we compared the GABA responses of neurons in acute slices from a-101.F-treated with control mice on P8. Consistent with cell culture results (Figure S5A), a-101.F-treated neurons retained a more depolarized value for E_{GABA} (Figures 3I–3K). To determine whether miR-101 regulation of NKCC1 mRNA alone was responsible for the delayed maturation of E_{GABA} , we employed an LNA target site blocker (TSB; Figures S5C and S5D). This is a novel and powerful strategy that allows the manipulation *in vivo* of a single miRNA-mRNA interaction without affecting the basal levels of mRNA targets. With this tool, we established a mechanistic link between the regulation of an individual mRNA and specific aspects of the phenotype induced by miRNA blockade. The NKCC1-TSB prevents binding of miR-101 to the miR-101 MRE in the 3' UTR of NKCC1, thereby freeing the transcript from miR-101 inhibitory regulation. All other miR-101 targets would still be subject to miR-101 repression; any pheno-

type observed would be exclusively due to NKCC1 de-repression. Injection of the NKCC1-TSB did indeed result in a higher level of the NKCC1 transcript (Figure S5D) and a more depolarized E_{GABA} , phenocopying the effect of a-101.F on the chloride gradient (Figures 3I–3K). The results clearly demonstrate that miR-101 directly suppresses NKCC1 levels and, thereby, promotes timely maturation of the chloride gradient to render GABA inhibitory. Maturation of the chloride gradient is an essential feature of early post-natal development whose initiation was not previously understood. A delay in this maturation, as in the case of miR-101 blockade, would be expected to have major consequences for the subsequent development of neural networks (Liu et al., 2006).

Protection of NKCC1 Alone Is Not Sufficient to Recapitulate a-101.F-Induced Network Dysfunction

When the hippocampal circuit is being established, large spontaneous synchronized events (SEs) are the major form of network activity (Ben-Ari, 2002; Blankenship and Feller, 2010; Bonifazi et al., 2009). SEs are generated by the concomitant action of depolarizing GABA and glutamate and are thought to drive synapse formation and help establish properly balanced local circuits (Cancedda et al., 2007; Deidda et al., 2015; Kirkby et al., 2013). Using calcium imaging, we tested whether the extended period of depolarized E_{GABA} induced by miR-101 blockade affected network dynamics. Acute hippocampal slices from a-101.F-treated P8 mice showed increased calcium transients relative to controls (Figures 4A–4C). SEs occurred more frequently and included larger cell ensembles (Figures 4D and 4E). Asynchronous events also occurred more frequently (Figure 4F). In addition, we observed other signs of hyper-excitability, as in the case of double SEs (i.e., two events occurring at a very short inter-event interval; Figure 4G) and saw large synchronous bursts (Figure S5E).

Consistent with a role for GABAergic excitation in promoting SEs (Blankenship and Feller, 2010; Bonifazi et al., 2009), disinhibition of NKCC1 alone (NKCC1-TSB), which prolongs the period of depolarizing GABA, was sufficient to replicate the effect of a-101.F on the frequency of SEs (Figure 4D). Importantly, NKCC1-TSB failed to replicate other aspects of the a-101.F phenotype, such as increases in the total number of events

(normalized first for β -actin and then for a-Ctrl fraction 1) for a-101.F yielded $F_1 = 1.65$, $F_2 = 1.95$, $F_3 = 0.15$, and $F_4 = 0.03$, whereas, for a-Ctrl, it yielded $F_1 = 1.00$, $F_2 = 1.35$, $F_3 = 0.02$, and $F_4 = 0.02$.

(D–F) Sensor technology was used to demonstrate *in vivo* that the NKCC1 miR-101 MRE affects protein expression levels.

(D) Top: scheme of the lentiviral construct showing a portion of the NKCC1 3' UTR cloned downstream of red fluorescent protein excited at 670nm (RFP₆₇₀). Bottom: sequence of the NKCC1 wild-type and the mutated miR-101 MREs.

(E) Images of the CA1 area from animals that received the wild-type (top) or the mutated NKCC1 sensor (bottom).

(F) Quantification of RFP₆₇₀ labeling, normalized to GFP, shows that the NKCC1 wild-type 3' UTR reduces RFP₆₇₀ fluorescence compared with a control sensor. The reduction is rescued when the miR-101 MRE is mutated.

(G and H) Loading hippocampal neurons in culture on days *in vitro* (DIV) 8 or 10 with fluorescent acetoxyethyl ester (Fluo-4AM) and challenging 1 hr later with GABA (in the presence of glutamate receptor blockers) revealed more responding cells when the cultures had been transfected with a-101. (Responding cells were defined as those having $\Delta F/F_0 \geq 50\%$ in response to GABA and are expressed as the percentage of all viable cells, as defined by those responding to 1 M KCl at the end of the recording). Images of loaded hippocampal neurons (G) and quantification of GABA responses (H).

(I–K) Antagonizing miR-101 (a-101.F) or protecting NKCC1 from miR-101 inhibition (NKCC1-TSB) delays E_{GABA} maturation *in vivo*.

(I) Gramicidin-perforated patch-clamp recordings of GABA-mediated currents from CA3 pyramidal neurons in P7–P8 hippocampal slices obtained at the indicated clamp potentials.

(J and K) Linear fit of current/voltage (I–V) plots used to estimate E_{GABA} (K) in CA3 neurons receiving a-Ctrl, a-101.F, or NKCC1-TSB. Scale bars, 100 pA, 200 ms. Bar graphs: mean \pm SEM, Student's t test, one-way ANOVA with Tukey's multiple comparison test (F and K); * $p < 0.05$, ** $p < 0.01$.

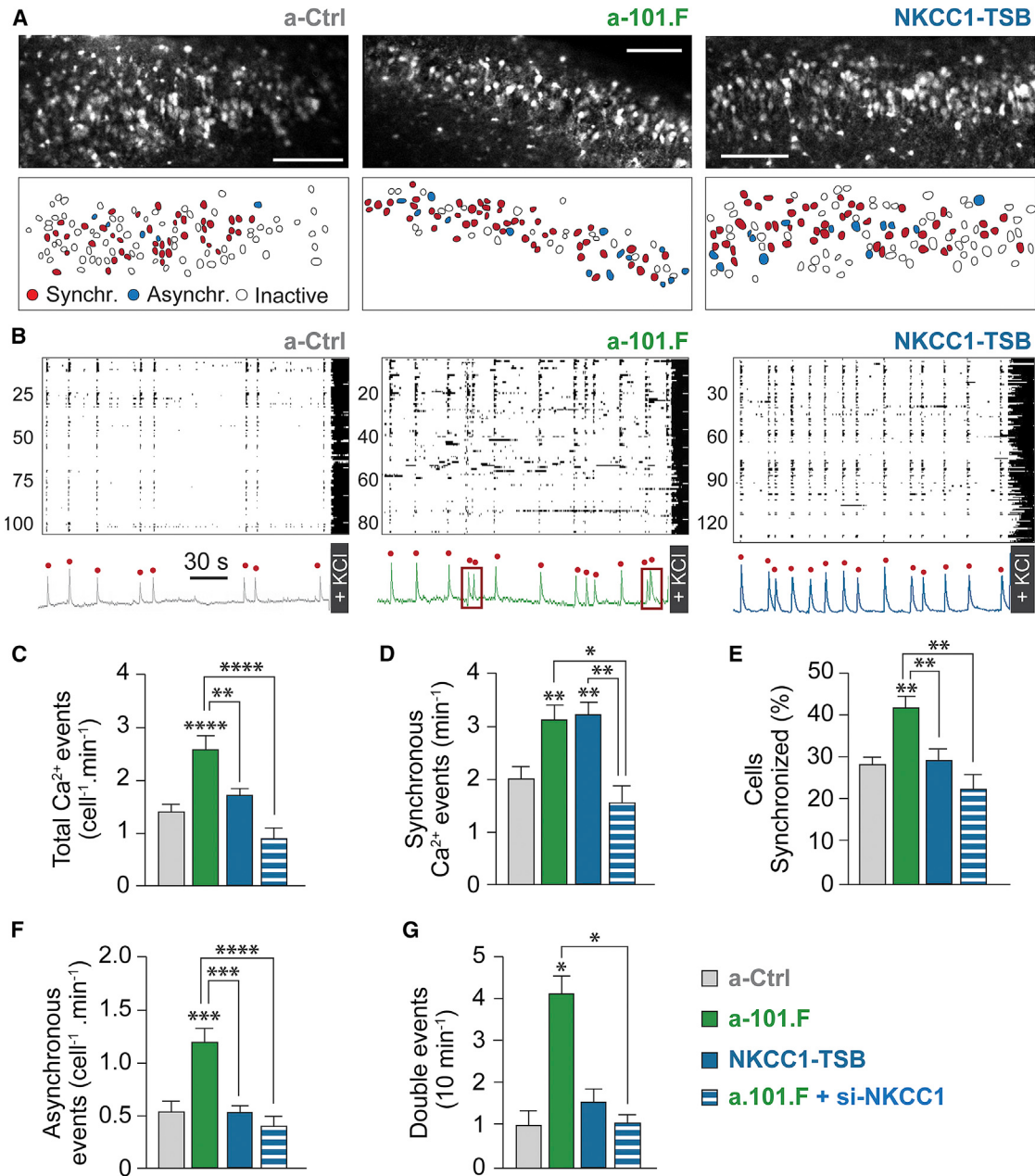


Figure 4. NKCC1-TSB Recapitulates Some, but Not All, Aspects of the a-101.F Phenotype

Shown is confocal imaging of spontaneous calcium transients in the CA3 region of acute P8 hippocampal slices.

(A) Images of CA3 from a-Ctrl- (left, top), a-101.F-treated (center, top), and NKCC1-TSB (right, top) mice showing cells participating in synchronous events (bottom, coded red), firing asynchronously (blue) or being inactive (showing only KCl-induced depolarization, white). Scale bars, 100 μm .

(B) Raster plots of activity in movies of a-Ctrl (left), a-101.F (center), and NKCC1-TSB (right) with principal component analyses of population activity shown below to identify synchronous events (red dots).

(C–G) MiR-101 inhibition increased the total number of events (C), including synchronous events (D), percentage of cells participating in synchronous events (E), incidence of asynchronous events (F), and frequency of double events (G, as shown in B, center, red boxes). Of these, de-repression of NKCC1 alone via NKCC1-TSB recapitulated only the effects on synchronous events (D). Partial knockdown of NKCC1 through an siRNA (si-NKCC1) co-injected with a-101.F completely rescued the entire phenotype induced by the absence of miR-101, indicating that NKCC1 expression is necessary, although not sufficient, for all aspects of the phenotype.

Bar graphs: mean \pm SEM, one-way ANOVA with Tukey's multiple comparison test; ** $p < 0.01$, *** $p < 0.001$, **** $p < 0.0001$.

(Figure 4C), the proportion of cells synchronized (Figure 4E), and the numbers of asynchronous events and double events (Figures 4F and 4G). Partial knockdown of NKCC1 with a small interfering RNA (siRNA) in the presence of a-101.F (Figure S5D), however, rescued the entire phenotype induced by a-101.F (Figures 4C–4G); this indicates that overexpression of NKCC1 is essential, although not sufficient, to generate all aspects of the a-101.F phenotype observed here. Taken together, the data indicate that NKCC1 repression by miR-101 is necessary to facilitate the GABA switch and to limit the frequency of SEs. Other miR-101 targets, however, must also be repressed to prevent excessive network activity.

MiR-101 Represses Multiple Programs in Parallel to Constrain Spontaneous Network Activity

To further elucidate the regulatory mechanisms by which miR-101 limits spontaneous activity, we examined six more candidates from the prioritized list (Table S1). We reasoned that multiple mRNA targets would have to be released simultaneously if we were to phenocopy all aspects of miR-101 blockade. Accordingly, we designed TSBs for each mRNA target and distributed them into three groups (G1, G2, and G3; Figure 5A), configured to maximize synergistic effects of the protected mRNAs while avoiding TSB combinations vulnerable to heteroduplex formation (Figure S6). All groups also contained NKCC1-TSB to ensure that the NKCC1 component of the phenotype was included as a baseline.

To assess their unique contributions, the groups were individually injected on P2, and their effects on spontaneous activity were monitored on P8 via calcium imaging. Remarkably, each group recapitulated unique aspects of the a-101.F phenotype not achieved by NKCC1-TSB alone (Figures 5B–5E and S7). The “presynaptic” G1 mimicked the increase in total activity primarily by increasing asynchronous events (Figures 5B and 5C). This is consistent with reports that Kif1a overexpression induces the formation of presynaptic boutons (Kondo et al., 2012) and that Ank2 stabilizes synapses (Bulat et al., 2014; Pielage et al., 2008). The “glia” G2 instead recapitulated the increase in the size of cell ensembles recruited in each synchronous event (Figure 5D). The finding is consistent with the role of Abca1 in meeting the high lipid demand of rapidly expanding membranes during dendritic growth and synaptogenesis (Table S1). The “neuronal excitability” G3 uniquely accounted for the large number of double events (Figure 5E). This may reflect the regulation of extrasynaptic glutamate by system xCT, thought to promote neuronal excitability in early circuits (Table S1). The selective effects of the groups on mRNA levels were confirmed by qPCR (Figure S7).

Because G1 phenocopied most aspects of a-101.F-induced changes in network activity, we further validated both Ank2 and Kif1a regulation by miR-101 (Figures S7 and S8). First, miR-101 inhibition was shown to increase protein levels (Figures S7G and S7H). Second, sensor assays were used to identify the miR-101 MREs for each and demonstrate specificity of the TSBs (Figure S8). Last, simultaneous knockdown of Ank2 and Kif1a (Figures 5F and 5G) was shown to rescue the increases in asynchronous and total calcium events (Figures 5I and 5J) induced by a-101.F but not the increase in SEs (Figure 5H).

The results indicate a specific role for the two presynaptic proteins in determining network activity.

An important feature of miR-101 revealed by a-101.F blockade is that actions during early post-natal life have lasting effects into adulthood. We hypothesized that the additional effects induced by G1, over and above that of NKCC1-TSB alone, could be sufficient to recapitulate the long-lasting effects on excitability seen with a-101.F. Indeed, calcium imaging in acute hippocampal slices prepared on P40 showed that G1, but not NKCC1-TSB, fully mimicked a-101.F in producing increased levels of activity and increased numbers of active cells in the DG (Figures 5K–5M), hallmarks of a hyper-excitable network.

The results indicate that miR-101 prevents excessive activity and that its actions early in development have lasting effects in the adult. It achieves this by repressing multiple developmental programs in parallel that control separate aspects of circuit formation, acting in different neuronal compartments and even in different cell types. Remarkably, protecting three core mRNA targets (NKCC1, Kif1a, and Ank2) from miR-101 regulation recapitulates the long-term hyper-excitability induced by a-101.F.

MiR-101 Targets Ank2 and Kif1a Complement NKCC1 in Constraining Synaptic Input

Having identified three core mRNA targets that miR-101 regulates to produce balanced networks, we then probed how they affect connectivity at the single-cell level. SEs and early spontaneous activity are known to guide synapse formation and network construction (Kirkby et al., 2013). Given that miR-101 blockade early in development increases spontaneous activity levels, we asked whether it affected synaptic input in a way likely to alter E/I. Recording from CA3 pyramidal neurons in P11 hippocampal acute slices revealed a clear increase in sEPSC frequency for animals receiving a-101.F on P2 compared with controls receiving a-Ctrl (Figures 6A and 6B). No change was seen in the spontaneous inhibitory postsynaptic current (sIPSC) frequency (Figure 6C) or in mean amplitude (Figures S9A and S9B). Importantly, the ratio of sEPSCs/sIPSCs was greatly increased, indicating an imbalance in E/I (Figure 6D). This suggests that the a-101.F-induced increase in early spontaneous network activity may have caused excessive synaptogenesis favoring excitatory input.

To test this hypothesis, we recorded miniature excitatory and inhibitory postsynaptic currents (mEPSCs and mIPSCs, respectively) from CA3 pyramidal neurons in acute P11 hippocampal slices. Because mEPSCs and mIPSCs represent the spontaneous release of individual synaptic vesicles in the absence of action potentials, their frequencies are often used to assess relative numbers of synaptic contacts (although other factors can sometimes also affect spontaneous release). Indeed, a-101.F increased the frequency of both mEPSCs and mIPSCs, consistent with increases in the numbers of both glutamatergic and GABAergic synapses (Figures 6E–6G, S9C, and S9D). No changes in mean amplitude were recorded (Figures S9E–S9H). Importantly, the increase in mEPSC frequency was proportionately greater, thereby increasing the ratio of mEPSC/mIPSC frequencies in a-101.F-treated animals (Figure 6H) and affecting E/I.

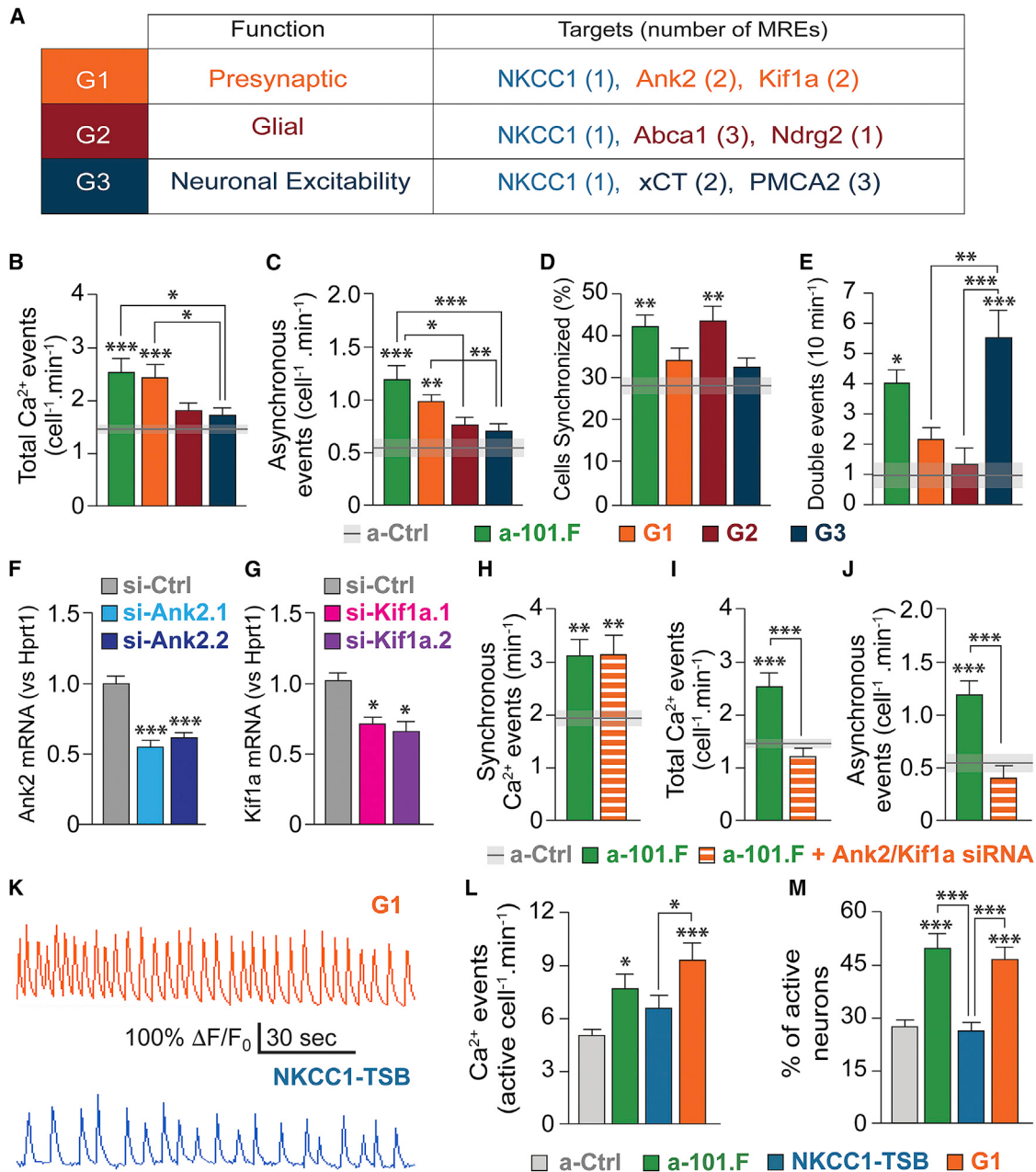


Figure 5. Additional mRNA Targets Must Be Protected to Reproduce the a.101.F Phenotype

(A) Grouping (left) of TSBs (right, numbers in brackets indicate the MREs for each mRNA) according to the general theme of the target (center). (B–E) Calcium imaging on P8 indicated that G1 uniquely recapitulates the increase in total activity (B) primarily because of more asynchronous events (C), G2 the increase in cells participating in SEs (D), and G3 the increase in double events (E). (F–J) Simultaneous knockdown of Ank2 and Kif1a rescues only certain aspects of the a-101.F phenotype. qPCR shows the effect of two siRNAs injected on P2 against Ank2 (si-Ank2, F) and Kif1a (si-Kif1a, G) levels on P8. Co-injection of siRNAs for Ank2 and Kif1a rescues the increase in frequency of total (I) and asynchronous (J) events but not of synchronous events (H) induced by a-101.F. (K–M) Calcium imaging on P40 revealed that network abnormalities persist in young adults receiving G1, but not NKCC1-TSB, on P2. Representative calcium traces (K). Quantification of calcium event frequency (L) and percentage of active cells (M). Bar graphs: mean \pm SEM, one-way ANOVA with Tukey's multiple comparison test (B–J), Kruskal Wallis with Dunn's multiple comparison test (L and M); *p < 0.05, **p < 0.01, ***p < 0.001.

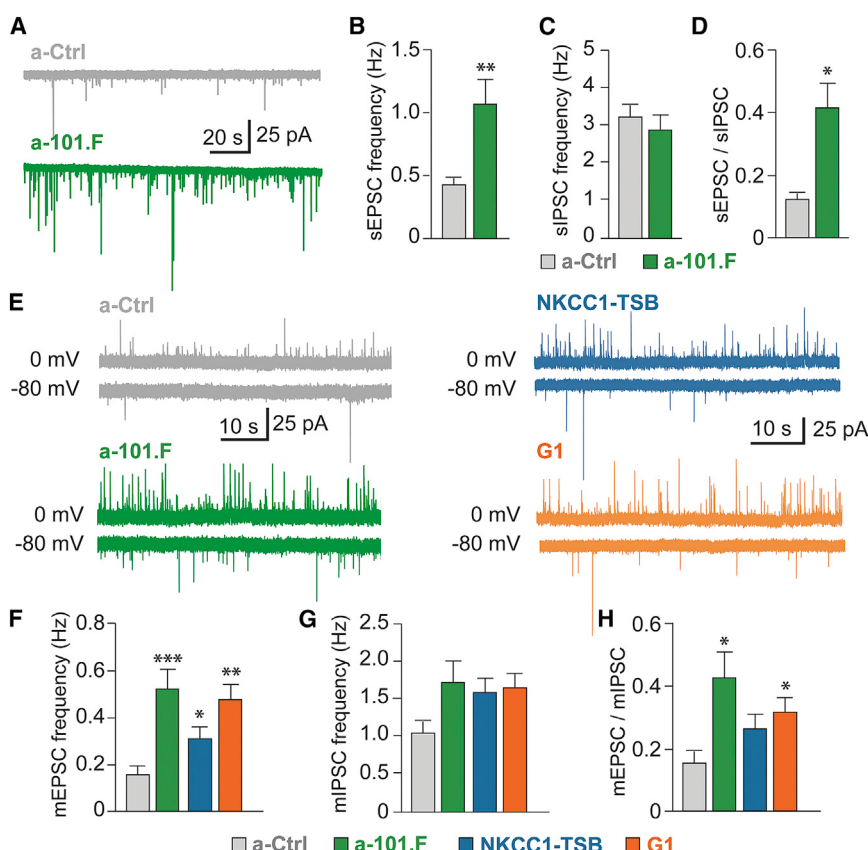


Figure 6. MiR-101 Targets NKCC1, Kif1a, and Ank2 to Restrain Synaptic Events and Balance E/I

(A) Recording sEPSCs in P11 acute hippocampal slices from a-Ctrl and a-101.F-treated mice.

(B–D) The a-101.F treatment increased the frequency of sEPSCs (B) but not sIPSCs (C), and, therefore, increased the ratio of sEPSCs/sIPSCs (D).

(E) Traces of mEPSCs (at -80 mV) and mIPSCs (at 0 mV) from a-Ctrl- (top, left), a-101.F-treated (bottom, left), NKCC1-TSB-treated (top, right), and G1-treated (bottom, right) animals.

(F–H) Both mEPSC (F) and mIPSC (G) frequencies were increased (see also Figure S9D), although mEPSCs proportionately more so by a-101.F, causing an increased mEPSC/mIPSC (H). G1 treatment better replicated a-101.F than NKCC1-TSB (F and H), indicating the additive effects of multiple pathways.

Bar graphs: mean ± SEM, one-way ANOVA with Tukey's multiple comparison test (B–D), Kruskal Wallis with Dunn's multiple comparison test (F–H); *p < 0.05, **p < 0.01, ***p < 0.001.

To identify the mechanisms by which specific miR-101 targets regulate synaptogenesis and determine E/I, we employed TSBs. We compared NKCC1-TSB, which completely recapitulates the increase in SEs induced by a-101.F, with G1, which phenocopies more closely the overall phenotype of a-101.F, including long-lasting effects. G1 was more effective than NKCC1-TSB alone in elevating mEPSC frequency on P11 (Figures 6E and 6F), whereas both yielded mIPSC frequencies equivalent to that of a-101.F (Figure 6G). As a result, G1 elevated the ratio of mEPSC/mIPSC frequencies, whereas NKCC1-TSB appeared to be less effective (Figure 6H).

The additional contributions of G1 were also apparent in the kinds of synaptic events seen. CA3 pyramidal neurons receive three major excitatory inputs that can be distinguished by analyzing the shape of individual synaptic events. mEPSCs with an amplitude greater than 30 pA almost exclusively originate from mossy fiber (MF) input (Henze et al., 1997). Compared with controls, a-101.F-treated animals showed an increase in the frequency of MF events (Figure S9I). G1-treated animals fully recapitulated this increase, whereas NKCC1-TSB-treated animals were not different from controls (Figure S9I). This suggests that both a-101.F and G1 induce an increase in the density of MF synapses (number per unit dendrite length), whereas NKCC1-TSB does not.

Other synaptic input to CA3 pyramidal neurons comes from commissural association fibers (A/Cs) and the perforant path where the mEPSC time to peak (TTP) is delayed because of den-

dritic filtering (Perez-Rosello et al., 2011). Examining mEPSCs smaller than 30 pA (to exclude MF synaptic events) yielded a slower TTP for NKCC1-TSB on average than for G1 (Figure S9J). This is consistent with proportionately more of the synaptic contacts being located farther away in the dendritic tree as a result of NKCC1-TSB treatment compared with G1.

NKCC1 and Kif1a/Ank2 Play Complementary Roles in Promoting Connectivity

Premature maturation of the GABA switch or selective local removal of depolarizing GABAergic input during development greatly reduces dendritic complexity (Cancedda et al., 2007; Chen and Kriegstein, 2015). This, together with the observation above that NKCC1-TSB increased the relative proportion of distal mEPSCs seen in CA3 pyramidal neurons without increasing MF events, suggested the hypothesis that release of NKCC1 from miR-101 regulation may preferentially enhance dendritic arbor complexity, whereas release of Ank2 and Kif1a may have a complementary effect in more directly promoting synaptic density.

To visualize changes in dendritic morphology, we co-injected the inhibitors on P2, along with a viral construct encoding EGFP, and then imaged CA1 and CA3 pyramidal proximal dendrites on P8 (Figure 7A). NKCC1-TSB alone fully matched the increases in length of primary dendritic branches produced by a-101.F in CA1 (Figures 7B and 7C) and both primary and secondary branches in CA3, whereas the branch number was unchanged (Figures S9K–S9M). G1 also recapitulated the a-101.F effect (data not shown), as expected, because it contains NKCC1-TSB. Previous work has shown that overexpression of Kif1a increases the number of presynaptic boutons (Kondo et al., 2012), whereas Ank2

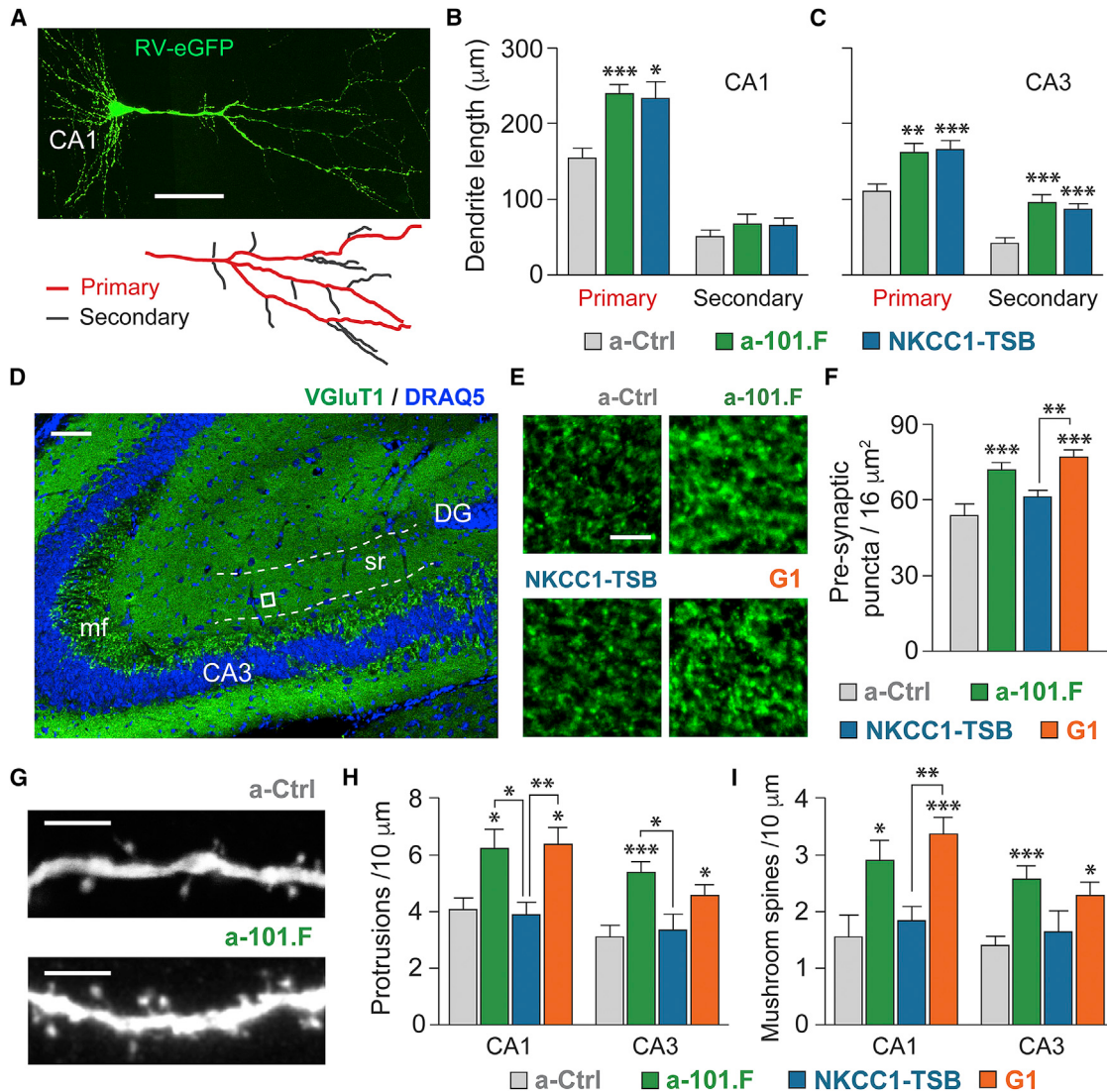


Figure 7. MiR-101 Repression of NKCC1 Restrains Dendritic Development, but Additional Targeting of Ank2 and Kif1a Is Necessary to Limit Formation of Presynaptic Puncta and Spinogenesis

(A) Sparse labeling of hippocampal pyramidal neurons with rabies virus expressing EGFP (top; scale bar, 50 μm) and characterization of dendritic morphology on P8 with NeuronJ (bottom).

(B and C) NKCC1-TSB recapitulates the increase in average dendritic length of CA1 primary (B) and CA3 primary and secondary dendrites (C) induced by miR-101.

(D) Presynaptic VGluT1 immunostaining in the stratum radiatum on P15 where CA3 A/Cs are prevalent. Scale bar, 50 μm .

(E and F) G1, but not NKCC1-TSB, recapitulates the increase induced by a-101.F. Scale bar, 5 μm . Representative images (E) of the area in CA3 used for the analysis (corresponding to the white box in D). Quantification of pre-synaptic puncta (F).

(G) Confocal imaging was used to analyze dendritic protrusions on primary proximal dendrites on P11. Scale bar, 5 μm .

(H and I) The increases in total protrusion density (H) and mushroom spine density (I) induced by a-101.F are phenocopied by G1 but not by NKCC1-TSB. Bar graphs: mean \pm SEM, one-way ANOVA with Tukey's multiple comparison test; * p < 0.05, ** p < 0.01, *** p < 0.001.

controls synapse stability (Bulat et al., 2014). To test whether these actions could explain mechanistically the difference between NKCC1-TSB and G1, we first immunostained for vesicular glutamate transporter (VGluT1) as a presynaptic marker of glutamatergic synapses. G1, but not NKCC1-TSB, was able to phenocopy, on P15, the increased numbers of puncta for VGluT1 seen in the stratum radiatum, where A/Cs are prevalent (Figures

7D–7F). The increase in VGluT1 presynaptic puncta induced by a-101.F injected on P2 was maintained on P30, a time when synapse formation and refinement are mostly completed (a-101.F had 1.6-fold more puncta than a-Ctrl, Student's t test, p < 0.01). Further, quantification on P11 of dendritic protrusions also revealed clear differences on the postsynaptic side. G1, but not NKCC1-TSB, mimicked the increased density of dendritic

protrusions both in the CA1 and CA3 seen with a-101.F (Figures 7G–7I). Notably, G1 also reproduced most closely the increase in “mushroom” spines, the type thought likely to represent mature glutamatergic synapses (Chen and Sabatini, 2012).

These results at the single-cell level elucidate the mechanistic details of how miR-101 curtails the development of excitatory input to generate a balanced network in the adult. Suppression of NKCC1 by miR-101 limits spontaneous activity and the activity-dependent genetic programs that promote dendritic growth. Repression of additional components (Kif1a/Ank2) is needed to constrain the formation of presynaptic boutons and the stabilization of synapses. Inhibition of these two developmental programs in parallel allows pyramidal neurons to receive appropriate excitatory input and avoid pathological levels of activity. Further, the fact that both CA1 and CA3 pyramidal cells are affected similarly by manipulation of miR-101 and its targets suggests that these are core mechanisms.

DISCUSSION

Creating robust neural networks with balanced E/I is essential for proper brain function, as evidenced by the many crippling neurological disorders reflecting deficiencies in this process. miRNAs are attractive candidates for coordinating the many pathways that must act in parallel during network formation to achieve a proper final balance. We show here that miR-101 performs such a role, inhibiting NKCC1, together with Ank2, Kif1a, and other mRNA targets, at a critical time during post-natal development to achieve optimal network excitability in the adult. Other miRNAs have previously been shown to regulate various aspects of neuronal development and morphology (Bian and Sun, 2011; Lippi et al., 2011; McNeill and Van Vactor, 2012; Schratt et al., 2006), but the present work represents a first in terms of identifying a single player orchestrating a comprehensive effect on neural circuit properties to maintain network stability long after the actual instruction.

MiR-101 Regulation of a Critical Phase in Network Development to Achieve a Balanced State

It has long been known that early post-natal neural development in rodents includes a period of exuberant growth that subsequently transitions into a phase of pruning and consolidation. This transition is when the fundamental properties of neural networks are established, including the general number and strength of synapses. Errors in the growth phase or in the timing of the transition have long-term consequences for network function (Cancedda et al., 2007; Chen and Kriegstein, 2015; Deidda et al., 2015; Dzhala et al., 2005; He et al., 2014; Liu et al., 2006). The elevation of miR-101 levels that occurs at this time suggested that it played a role; specific blockade of miR-101 by injection of a-101.F on P2 confirmed it. The blockade produced profound changes in network excitability and behavior that persisted well into adulthood. Importantly, these effects were driven exclusively by miR-101 events in early post-natal life because the blockade achieved by a-101.F expired within 9 days of injection, as evidenced by qPCR of both the miR and its targets. Further, blockade of miR-101 in the adult did not replicate any of these effects, indicating that its expression in the

adult must serve other purposes (Lee et al., 2008; Vilardo et al., 2010). The results permit the unambiguous conclusion that early miR-101 action has long-lasting effects. This outcome is quite different from those reported previously for miRNA actions in the nervous system, such as those of miR-128, which appears to act in the adult to regulate ion channels and ERK2 signaling pathways (Tan et al., 2013). The fact that high levels of miR-101 have also been found in the cortex at the end of the second week of post-natal life (Chi et al., 2009) suggests a global role in the developing brain that merits further investigation.

Coordination of Distinct Programs by MiR-101 for a Common Purpose

The ability of miR-101 to coordinate the development of a major brain feature (i.e., balanced networks) by regulating key independent programs in parallel is well illustrated by its actions on pyramidal neurons in the hippocampus. During development, the neurons elaborate extensive dendritic branches and receive large numbers of synaptic contacts. This development depends in part on local GABAergic signaling initially being depolarizing. Selective silencing of that GABAergic input (Chen and Kriegstein, 2015) or accelerated maturation of the chloride gradient to render GABA inhibitory impairs dendritic arborization (Cancedda et al., 2007). Conversely, TSB protection of NKCC1 against miR-101 regulation prolongs the period of depolarizing GABA and increases the frequency of SEs, triggering activity-dependent gene programs that induce the neurons to extend longer dendritic branches. The additional protection of Ank2 and Kif1a obtained by G1, however, is required to increase the density of synapses formed on the branches, as seen immunohistochemically.

Previous studies have suggested roles for Ank2 and Kif1a in synapse formation or stabilization (Bulat et al., 2014; Koch et al., 2008; Kondo et al., 2012; Pielage et al., 2008; Stephan et al., 2015; Yonekawa et al., 1998). Consistent with this, G1, which protects Ank2 and Kif1a along with NKCC1, increased both the density of VGluT1-containing presynaptic puncta and the density of dendritic protrusions, whereas NKCC1-TSB affected only dendritic arborization. The overall outcome is that G1, but not NKCC1-TSB alone, causes an imbalance in E/I and produces long-lasting hyper-excitability. Notably, G2 and G3 contain TSBs protecting yet other miR-101 targets responsible for unique aspects of the changes in spontaneous network activity induced by a-101.F. An interesting question for the future is whether G2 and G3 may recapitulate pathological aspects of a-101.F that were not detected in G1-treated adults, such as the SLE and excitatory bursts.

Perhaps surprisingly, miR-101 does not appear to regulate KCC2, although a developmental increase in KCC2 during the second week of post-natal life normally complements the decrease in NKCC1 to execute maturation of the chloride gradient (Ben-Ari, 2002; Blankenship and Feller, 2010; Rivera et al., 1999). MiR-101 does not, for example, target any components of the RE1-silencing transcription factor (REST) complex, a repressor that inhibits KCC2 early in development (Karadsheh and Delpire, 2001), before transcription factors potently induce its expression (Medina et al., 2014). Upstream events are most

likely responsible, coordinating the repression of NKCC1 via miR-101 while releasing expression of KCC2 through other mechanisms.

The results clearly demonstrate that miR-101 regulates multiple developmental programs at a critical early stage to achieve the goal of a stable, balanced network in the adult. It does this by constraining the growth phase and facilitating the transition to consolidation, thereby limiting the development of excitatory input. Importantly, blockade of these miR-101 actions does not simply delay development; instead, it causes persistent deficits that apparently cannot be fully compensated even in adulthood. In addition to the targets identified here, miR-101 almost certainly regulates many other mRNAs simultaneously to produce the global effect of controlling E/I and stabilizing network function. The candidate approach utilized in this work, in particular the use of TSBs, should also be effective in parsing out additional contributions of other targets repressed by miR-101.

Pathological Consequences and Behavioral Relevance

Previous studies have linked miR-101 to various neurological disorders because of its regulation of specific targets, as in the case of Atxn1 in spinocerebellar ataxia type I (Lee et al., 2008) and the amyloid precursor protein in Alzheimer's disease (Vilardo et al., 2010). In contrast, our findings define a much broader role for miR-101 in neural development, coordinating multiple pathways in early post-natal life to achieve long-lasting network stability. Disruption of miR-101 action causes hyper-excitability and cognitive impairments. These pathological outcomes reflect features common to many neurodevelopmental disorders (Bellforte et al., 2010; Chao et al., 2010; Rubenstein and Merzenich, 2003; Yizhar et al., 2011; Zoghbi and Bear, 2012) in which miRNA dysfunctions have often been reported (Im and Kenny, 2012; Wu et al., 2016).

Interestingly, several of the miR-101 targets identified here have been linked to specific features of neurodevelopmental disorders. NKCC1 and the maturation of the chloride gradient have been linked to seizure susceptibility (Dzhala et al., 2005). Kif1a mutations in humans cause cognitive impairment, atrophy, neuropathy, and epilepsy (Lee et al., 2015). Both Slc7a11 and Ank2 belong to modules of ASD risk genes that have a key role in neural development and in establishing connectivity of glutamatergic neurons; they are themselves regulated by the fragile X mental retardation protein (FMRP; Parikshak et al., 2013; Voineagu et al., 2011). Notably, miR-101 levels are altered in patients with ASD (Mundallil Vasu et al., 2014) and schizophrenia (Beveridge et al., 2010). MiR-101 has also been linked to fragile X syndrome (Zongaro et al., 2013) because of its ability to regulate FMRP, and it has been connected to Rett syndrome because it is responsive to the transcriptional regulator Mecp2, which, in mutated form, can cause Rett syndrome (Wu et al., 2010). These reports indicate the biomedical relevance of the regulatory cascades controlled by miR-101.

Taken together, these findings suggest that miR-101 regulates a highly interconnected gene network that controls the phase of initial growth in neural nets, the strength of excitatory input within them, and its balance with inhibition. Our work provides new insight into brain development and reveals potential targets for

therapeutic intervention to compensate or reverse multiple disease states.

EXPERIMENTAL PROCEDURES

Animals

Animals were housed under 12/12 hr light/dark cycle (7:00 a.m.–7:00 p.m.) at 23°C ± 1°C with free access to food and water. All experimental procedures at UCSD were performed as approved by the Institutional Animal Care and Use Committee and according to the NIH Guidelines for the Care and Use of Laboratory Animals. Behavioral and *in vivo* experiments at UNIMORE were conducted in accordance with the European Community Council Directive (86/609/EEC) of November 24, 1986, and approved by the ethics committee.

RNA Sequencing and qPCR

miRNA analysis was performed as described previously (Zisoulis et al., 2010), and sequencing was based on Illumina's Small RNA Digital Gene Expression v1.5 protocol. Semiquantitative PCR was used to measure miRNA levels and their mRNA targets in RNA from dorsal hippocampus or hippocampal slices as described previously (Lippi et al., 2011) using the miRNeasy mini kit (QIAGEN). Both here and below, see the *Supplemental Experimental Procedures* for details.

Behavior

Animals received LNAs or viral constructs on P2 and, after reaching 8 weeks, were subjected to a battery of behavioral tests using standard procedures as described.

Electrical Recordings

In vivo single-unit recording was performed with implanted microdrive recording devices using electrode assemblies with four tetrodes. Single units were isolated, and firing rates were determined for periods when animals were quietly resting (characterized by the absence of a hippocampal theta rhythm). Histological analysis of serial sections was used to confirm electrode positions in the cornu Ammonis (CA) cell layers.

Patch-clamp recording from neurons in acute slices was performed using standard techniques. To determine E_{GABA} , perforated patch-clamp recordings were obtained with gramicidin in the patch electrode.

Calcium Imaging

Calcium imaging was performed on neurons in acute slices on P8 after loading with calcium fluor. Imaging on P40 was performed using virally encoded GCaMP6 co-injected on P2 with LNA antagonists. A custom-made MATLAB pipeline was used for analysis.

SUPPLEMENTAL INFORMATION

Supplemental Information includes Supplemental Experimental Procedures, nine figures, and one table and can be found with this article online at <http://dx.doi.org/10.1016/j.neuron.2016.11.017>.

AUTHOR CONTRIBUTIONS

G.L., A.B.J., E.P.F., S.R.T., J.C.L., and M.M.C. performed calcium imaging experiments. C.C.F. and D.J. performed electrophysiological experiments. J.L.N. and G.W.Y. performed small RNA sequencing. L.A.E., J.K.L., and G.L. performed *in vivo* recordings. B.R., G.C., G.B., and M.Z. performed behavioral tests and MES tests. E.P.F. wrote the code for calcium imaging analysis. C.B. performed western blot analysis. G.L. performed all remaining experiments. G.L. and D.K.B. wrote the paper. All authors performed data analysis and reviewed and commented on versions of the manuscript.

ACKNOWLEDGMENTS

We thank E. Terenziani, H. Andrews, E. Ng, I. Lai, and H. Zhang for help with calcium imaging analysis; X. Wang for LNA injections; M. Lippi for helping

with the analysis code; L. Manca, A. Tombesi, and A. Vilella for technical assistance with *in situ* hybridization experiments; V. Jayaraman and K. Svoboda from the GENIE Project for providing the AAV GCaMP6f; and C. Barbato and F. Ruberti for reagents. We thank N.C. Spitzer, M. Scanziani, S. Leutgeb, W.B. Kristan, and D. Dulcis for reviewing versions of the manuscript. This work was supported by grants from the NIH (2R01NS012601 and 1R21NS087342), TRDRP (22XT-0016, 21FT-0027, and 25IP-0019), and UNIMORE FAR2014 (to M.Z.). A.B.J. was supported by the Lundbeck Foundation.

Received: April 25, 2016

Revised: October 7, 2016

Accepted: November 3, 2016

Published: December 8, 2016

REFERENCES

- Bartel, D.P. (2004). MicroRNAs: genomics, biogenesis, mechanism, and function. *Cell* 116, 281–297.
- Belforte, J.E., Zsiros, V., Sklar, E.R., Jiang, Z., Yu, G., Li, Y., Quinlan, E.M., and Nakazawa, K. (2010). Postnatal NMDA receptor ablation in corticolimbic interneurons confers schizophrenia-like phenotypes. *Nat. Neurosci.* 13, 76–83.
- Ben-Ari, Y. (2002). Excitatory actions of gaba during development: the nature of the nurture. *Nat. Rev. Neurosci.* 3, 728–739.
- Beveridge, N.J., Gardiner, E., Carroll, A.P., Tooney, P.A., and Cairns, M.J. (2010). Schizophrenia is associated with an increase in cortical microRNA biogenesis. *Mol. Psychiatry* 15, 1176–1189.
- Bian, S., and Sun, T. (2011). Functions of noncoding RNAs in neural development and neurological diseases. *Mol. Neurobiol.* 44, 359–373.
- Blankenship, A.G., and Feller, M.B. (2010). Mechanisms underlying spontaneous patterned activity in developing neural circuits. *Nat. Rev. Neurosci.* 11, 18–29.
- Bonifazi, P., Goldin, M., Picardo, M.A., Jorquera, I., Cattani, A., Bianconi, G., Represa, A., Ben-Ari, Y., and Cossart, R. (2009). GABAergic hub neurons orchestrate synchrony in developing hippocampal networks. *Science* 326, 1419–1424.
- Boudreau, R.L., Jiang, P., Gilmore, B.L., Spengler, R.M., Tirabassi, R., Nelson, J.A., Ross, C.A., Xing, Y., and Davidson, B.L. (2014). Transcriptome-wide discovery of microRNA binding sites in human brain. *Neuron* 81, 294–305.
- Bulat, V., Rast, M., and Pielage, J. (2014). Presynaptic CK2 promotes synapse organization and stability by targeting Ankyrin2. *J. Cell Biol.* 204, 77–94.
- Cancedda, L., Fiumelli, H., Chen, K., and Poo, M.M. (2007). Excitatory GABA action is essential for morphological maturation of cortical neurons *in vivo*. *J. Neurosci.* 27, 5224–5235.
- Chao, H.T., Chen, H., Samaco, R.C., Xue, M., Chahrour, M., Yoo, J., Neul, J.L., Gong, S., Lu, H.C., Heintz, N., et al. (2010). Dysfunction in GABA signalling mediates autism-like stereotypies and Rett syndrome phenotypes. *Nature* 468, 263–269.
- Chen, J., and Kriegstein, A.R. (2015). A GABAergic projection from the zona incerta to cortex promotes cortical neuron development. *Science* 350, 554–558.
- Chen, Y., and Sabatini, B.L. (2012). Signaling in dendritic spines and spine microdomains. *Curr. Opin. Neurobiol.* 22, 389–396.
- Chi, S.W., Zang, J.B., Mele, A., and Darnell, R.B. (2009). Argonaute HITS-CLIP decodes microRNA-mRNA interaction maps. *Nature* 460, 479–486.
- Curzon, P., Rustay, N.R., and Brownman, K.E. (2009). Cued and contextual fear conditioning for rodents. In Methods of Behavior Analysis in Neuroscience, Second Edition, J.J. Buccafusco, ed. (CRC Press/Taylor & Francis).
- Deidda, G., Allegra, M., Cerri, C., Naskar, S., Bony, G., Zunino, G., Bozzi, Y., Caleo, M., and Cancedda, L. (2015). Early depolarizing GABA controls critical-period plasticity in the rat visual cortex. *Nat. Neurosci.* 18, 87–96.
- Dzhala, V.I., Talos, D.M., Sdrulla, D.A., Brumback, A.C., Mathews, G.C., Benke, T.A., Delpire, E., Jensen, F.E., and Staley, K.J. (2005). NKCC1 transporter facilitates seizures in the developing brain. *Nat. Med.* 11, 1205–1213.
- Guo, H., Ingolia, N.T., Weissman, J.S., and Bartel, D.P. (2010). Mammalian microRNAs predominantly act to decrease target mRNA levels. *Nature* 466, 835–840.
- He, Q., Nomura, T., Xu, J., and Contractor, A. (2014). The developmental switch in GABA polarity is delayed in fragile X mice. *J. Neurosci.* 34, 446–450.
- Henze, D.A., Card, J.P., Barrionuevo, G., and Ben-Ari, Y. (1997). Large amplitude miniature excitatory postsynaptic currents in hippocampal CA3 pyramidal neurons are of mossy fiber origin. *J. Neurophysiol.* 77, 1075–1086.
- Im, H.I., and Kenny, P.J. (2012). MicroRNAs in neuronal function and dysfunction. *Trends Neurosci.* 35, 325–334.
- Karadshian, M.F., and Delpire, E. (2001). Neuronal restrictive silencing element is found in the KCC2 gene: molecular basis for KCC2-specific expression in neurons. *J. Neurophysiol.* 85, 995–997.
- Kirkby, L.A., Sack, G.S., Firl, A., and Feller, M.B. (2013). A role for correlated spontaneous activity in the assembly of neural circuits. *Neuron* 80, 1129–1144.
- Koch, I., Schwarz, H., Beuchle, D., Goellner, B., Langegger, M., and Aberle, H. (2008). Drosophila ankyrin 2 is required for synaptic stability. *Neuron* 58, 210–222.
- Kondo, M., Takei, Y., and Hirokawa, N. (2012). Motor protein KIF1A is essential for hippocampal synaptogenesis and learning enhancement in an enriched environment. *Neuron* 73, 743–757.
- Lee, Y., Samaco, R.C., Gatchel, J.R., Thaller, C., Orr, H.T., and Zoghbi, H.Y. (2008). miR-19, miR-101 and miR-130 co-regulate ATXN1 levels to potentially modulate SCA1 pathogenesis. *Nat. Neurosci.* 11, 1137–1139.
- Lee, J.R., Srour, M., Kim, D., Hamdan, F.F., Lim, S.H., Brunel-Guitton, C., Décarie, J.C., Rossignol, E., Mitchell, G.A., Schreiber, A., et al. (2015). De novo mutations in the motor domain of KIF1A cause cognitive impairment, spastic paraparesis, axonal neuropathy, and cerebellar atrophy. *Hum. Mutat.* 36, 69–78.
- Lippi, G., Steinert, J.R., Marcylo, E.L., D’Oro, S., Fiore, R., Forsythe, I.D., Schratt, G., Zoli, M., Nicotera, P., and Young, K.W. (2011). Targeting of the Arpc3 actin nucleation factor by miR-29a/b regulates dendritic spine morphology. *J. Cell Biol.* 194, 889–904.
- Liu, Z., Neff, R.A., and Berg, D.K. (2006). Sequential interplay of nicotinic and GABAergic signaling guides neuronal development. *Science* 314, 1610–1613.
- Makeyev, E.V., Zhang, J., Carrasco, M.A., and Maniatis, T. (2007). The microRNA miR-124 promotes neuronal differentiation by triggering brain-specific alternative pre-mRNA splicing. *Mol. Cell* 27, 435–448.
- McNeill, E., and Van Vactor, D. (2012). MicroRNAs shape the neuronal landscape. *Neuron* 75, 363–379.
- Medina, I., Friedel, P., Rivera, C., Kahle, K.T., Kourdougli, N., Uvarov, P., and Pellegrino, C. (2014). Current view on the functional regulation of the neuronal K(+)-Cl(-) cotransporter KCC2. *Front. Cell. Neurosci.* 8, 27.
- Mundalil Vasu, M., Anitha, A., Thanseem, I., Suzuki, K., Yamada, K., Takahashi, T., Wakuda, T., Iwata, K., Tsujii, M., Sugiyama, T., and Mori, N. (2014). Serum microRNA profiles in children with autism. *Mol. Autism* 5, 40.
- Parikhshak, N.N., Luo, R., Zhang, A., Won, H., Lowe, J.K., Chandran, V., Horvath, S., and Geschwind, D.H. (2013). Integrative functional genomic analyses implicate specific molecular pathways and circuits in autism. *Cell* 155, 1008–1021.
- Perez-Rosello, T., Baker, J.L., Ferrante, M., Iyengar, S., Ascoli, G.A., and Barrionuevo, G. (2011). Passive and active shaping of unitary responses from associational/commissural and perforant path synapses in hippocampal CA3 pyramidal cells. *J. Comput. Neurosci.* 31, 159–182.
- Pielage, J., Cheng, L., Fetter, R.D., Carlton, P.M., Sedat, J.W., and Davis, G.W. (2008). A presynaptic giant ankyrin stabilizes the NMJ through regulation of presynaptic microtubules and transsynaptic cell adhesion. *Neuron* 58, 195–209.
- Rivera, C., Voipio, J., Payne, J.A., Ruusuvuori, E., Lahtinen, H., Lamsa, K., Pirvola, U., Saarma, M., and Kaila, K. (1999). The K+/Cl- co-transporter KCC2 renders GABA hyperpolarizing during neuronal maturation. *Nature* 397, 251–255.

- Rubenstein, J.L., and Merzenich, M.M. (2003). Model of autism: increased ratio of excitation/inhibition in key neural systems. *Genes Brain Behav.* 2, 255–267.
- Schratt, G.M., Tuebing, F., Nigh, E.A., Kane, C.G., Sabatini, M.E., Kiebler, M., and Greenberg, M.E. (2006). A brain-specific microRNA regulates dendritic spine development. *Nature* 439, 283–289.
- Stephan, R., Goellner, B., Moreno, E., Frank, C.A., Hugenschmidt, T., Genoud, C., Aberle, H., and Pielage, J. (2015). Hierarchical microtubule organization controls axon caliber and transport and determines synaptic structure and stability. *Dev. Cell* 33, 5–21.
- Tan, C.L., Plotkin, J.L., Venø, M.T., von Schimmelmann, M., Feinberg, P., Mann, S., Handler, A., Kjems, J., Surmeier, D.J., O'Carroll, D., et al. (2013). MicroRNA-128 governs neuronal excitability and motor behavior in mice. *Science* 342, 1254–1258.
- Vilardo, E., Barbato, C., Ciotti, M., Cogoni, C., and Ruberti, F. (2010). MicroRNA-101 regulates amyloid precursor protein expression in hippocampal neurons. *J. Biol. Chem.* 285, 18344–18351.
- Voineagu, I., Wang, X., Johnston, P., Lowe, J.K., Tian, Y., Horvath, S., Mill, J., Cantor, R.M., Blencowe, B.J., and Geschwind, D.H. (2011). Transcriptomic analysis of autistic brain reveals convergent molecular pathology. *Nature* 474, 380–384.
- Wu, H., Tao, J., Chen, P.J., Shahab, A., Ge, W., Hart, R.P., Ruan, X., Ruan, Y., and Sun, Y.E. (2010). Genome-wide analysis reveals methyl-CpG-binding protein 2-dependent regulation of microRNAs in a mouse model of Rett syndrome. *Proc. Natl. Acad. Sci. USA* 107, 18161–18166.
- Wu, Y.E., Parikshak, N.N., Belgard, T.G., and Geschwind, D.H. (2016). Genome-wide, integrative analysis implicates microRNA dysregulation in autism spectrum disorder. *Nat. Neurosci.* 19, 1463–1476.
- Yizhar, O., Fenn, L.E., Prigge, M., Schneider, F., Davidson, T.J., O'Shea, D.J., Sohal, V.S., Goshen, I., Finkelstein, J., Paz, J.T., et al. (2011). Neocortical excitation/inhibition balance in information processing and social dysfunction. *Nature* 477, 171–178.
- Yonekawa, Y., Harada, A., Okada, Y., Funakoshi, T., Kanai, Y., Takei, Y., Terada, S., Noda, T., and Hirokawa, N. (1998). Defect in synaptic vesicle precursor transport and neuronal cell death in KIF1A motor protein-deficient mice. *J. Cell Biol.* 141, 431–441.
- Yoo, A.S., Staahl, B.T., Chen, L., and Crabtree, G.R. (2009). MicroRNA-mediated switching of chromatin-remodelling complexes in neural development. *Nature* 460, 642–646.
- Zisoulis, D.G., Lovci, M.T., Wilbert, M.L., Hutt, K.R., Liang, T.Y., Pasquinelli, A.E., and Yeo, G.W. (2010). Comprehensive discovery of endogenous Argonaute binding sites in *Caenorhabditis elegans*. *Nat. Struct. Mol. Biol.* 17, 173–179.
- Zoghbi, H.Y., and Bear, M.F. (2012). Synaptic dysfunction in neurodevelopmental disorders associated with autism and intellectual disabilities. *Cold Spring Harb. Perspect. Biol.* 4, a009886.
- Zongaro, S., Hukema, R., D'Antoni, S., Davidovic, L., Barbry, P., Catania, M.V., Willemsen, R., Mari, B., and Bardoni, B. (2013). The 3' UTR of FMR1 mRNA is a target of miR-101, miR-129-5p and miR-221: implications for the molecular pathology of FXTAS at the synapse. *Hum. Mol. Genet.* 22, 1971–1982.